FATIGUE AND CRACK PROPAGATION STUDY IN THE KNEE LOCKING MECHANISM OF A SEMI-AUTOMATIC BLOWING MACHINE

Abdallah DJENNANE[11*], Kamel ZIDANI[2], Rachid BENBOUTA[3]

This study investigates the fatigue degradation and crack propagation in the locking mechanism of PET bottle blow molding machines, focusing on the impact of elliptical cracks on the mechanism's performance and longevity. The locking mechanism, which plays a vital role in securing the mold during the blow molding process, is subjected to repeated loading, making it susceptible to fatigue damage. Using a combination of finite element analysis (FEA) and experimental methodologies, we examine the stress distribution, deformation, and displacement in the mechanism under operational loads. The study identifies the most stressed component and models the behavior of an elliptical crack located at the center of this component. A stress intensity factor (K) of 3.7553 MPa.mm$^{-0.5}$ is found, indicating significant risk in the crack region. Fatigue analysis using Goodman's law predicts a service life of one million cycles with a safety factor of 2.08. These findings highlight the need for targeted design and maintenance strategies to enhance the reliability and durability of PET blow molding machines.

Keywords: Blow molding machines, Locking mechanism, Bottle Blow, Metal fatigue, Epileptic cracks, Stress intensity factor.

1. Introduction

The blow molding process is used to manufacture hollow bodies, such as bottles or flasks. The blow molding process is mainly used for thermoplastic materials, such as polypropylene (PP) or polylactide (PLA). Today, however, polyethylene terephthalate (PET) is still the most widely used polymer for blow-molded bottles [1].

The soft drinks industry is growing steadily, leading to increased demand for PET bottles. PET bottle blow molders are essential machines for the production of these bottles. The locking mechanism on these machines plays a crucial role in ensuring that the mold is securely closed during the blow molding process.

[1] Lecturer, LRP Laboratory, Dept. of Mechanical Engineering, University of BATNA 2, Algeria, e-mail: abdellah.djenane@univ-batna2.dz;
[2] Prof., LICEGS Laboratory, Dept. of Mechanical Engineering, University of BATNA 2, Algeria
[3] Prof., LICEGS Laboratory, Dept. of Mechanical Engineering, University of BATNA 2, Algeria
e-mail: r.benbouta@univ-batna2.dz

However, this mechanism is subjected to repeated loads during operation, which can lead to fatigue degradation and cracking. Fatigue is a mechanical phenomenon that occurs when a material is subjected to cyclic or fluctuating loads. Over time, these loads can lead to the formation of micro-cracks in the material, which can propagate and eventually lead to catastrophic failure [2].

The presence of elliptical cracks in the locking mechanism of a PET bottle blow molder can pose a significant risk to the safety and reliability of the machine. From the standpoint of numerical modeling, the primary challenge lies in the extensive number of load cycles, which significantly increases computational demands. Additionally, the understanding of the underlying mechanisms of the fatigue phenomenon is still insufficient. Fatigue involves numerous complex processes occurring across various scales. Consequently, several numerical approaches to fatigue rely on well-established phenomenological laws. For example, the Paris law is used to model fatigue crack propagation through finite elements and generalized finite elements, as shown by the work of Judt et al. [3] and O'Hara et al. [4]. These results are then used to develop a numerical model of the phenomenon. This law is also a key component of NASGRO, a widely used tool for fatigue crack growth simulations [5]. However, other works [6, 7] have addressed the modeling of cyclic fatigue life up to crack initiation using the continuum damage mechanics (CDM) framework developed by [8]. Fish and Oskay [9] proposed a numerical model in which the damage evolution is represented by an increasing void volume fraction, governed by the Gurson model. In their approach, cracks are simulated by the suppression of finite elements when the void volume fraction exceeds a critical damage threshold. Generally, accurately approximating cracks or crack growth within a conventional simulation framework is challenging, as it requires the integration of element deletion or remeshing algorithms. A highly effective technique to address these issues is the phase field method. This method models cracks using an additional scalar field that distinguishes between broken and intact material. This scalar field is coupled to material stiffness, thus allowing modeling the substantial reduction in stiffness in damaged areas. Over the past decade, the phase field method has gained significant attention, leading to numerous studies across various fields of fracture mechanics. These studies encompass a wide range of topics, from dynamic fracture [10] and brittle fracture [11, 12] to ductile fracture [13-15] and models incorporating the effects of anisotropic materials [16, 17].

In the mentioned works, almost all authors have extensively studied the fatigue degradation and crack propagation in various mechanical components using numerical and experimental methodologies. However, these studies often focus on simpler geometries or materials and may not adequately address the complexities involved in the locking mechanisms of PET bottle blow molding machines. Specifically, the presence of elliptical cracks and their impact on the

fatigue life of such mechanisms have not been thoroughly investigated. In our paper, we address these gaps by developing a comprehensive experimental and numerical methodology to analyze the fatigue degradation of the locking mechanism in PET bottle blow molding machines. Our approach involves detailed stress distribution and crack propagation analysis, taking into accounts the unique operational loads and material properties of the locking mechanism. We successfully model the behavior of an elliptical crack within the most stressed component of the system, providing insights into the stress distribution, deformation, and displacement under various loading conditions.

This study makes a significant contribution to improving the reliability and durability of PET blow molding machines. By combining in-depth theoretical analyses and numerical simulations, it enables the development of tools for predicting component lifespan and optimizing maintenance strategies. The results of this study are likely to have a positive impact on the entire packaging industry.

To take this research further, it would be interesting to integrate artificial intelligence. Using machine learning techniques could enable the development of even more accurate and robust lifespan prediction models.

2. Description of the structure of the blow-molding machine

The mechanical structure of the blower unit is compact and optimized, with dimensions of 1.5 × 0.7 × 1.6 meters, making it suitable for industrial production lines (Figs. 1 and 2). It operates using integrated electro-pneumatic systems that ensure precise process control. Designed for manufacturing plastic bottles ranging from 0.5 to 2 liters, it offers a production capacity of 1000 to 1200 bottles per hour.

The operating cycle includes preheating the preforms, mechanical stretching, and high-pressure blowing (up to 40 bar). The machine is controlled by a PLC-based control panel, allowing automation, monitoring, and parameter adjustments, within an ambient temperature range of 15 to 35 °C.

The machine includes a stretching unit, a mold closing mechanism, a parallel clamping system, and an air reservoir. Its base structure, made of folded sheet metal, ensures strength and durability, while the auxiliary welded frame supports the access panels and control area. The latter contains the electro-pneumatic interface components. The parallel clamping system ensures uniform pressure on the mold, while the stretching unit improves material distribution. The air reservoir stabilizes pressure and ensures rapid blowing.

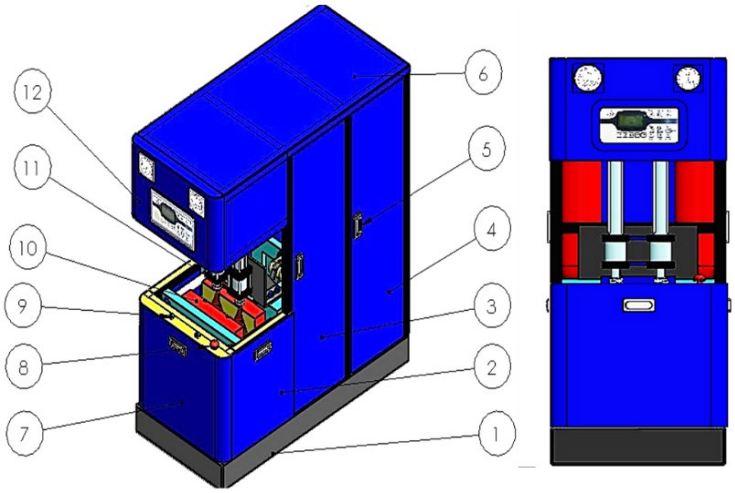

Fig. 1. CAD model of the blow-molding machine

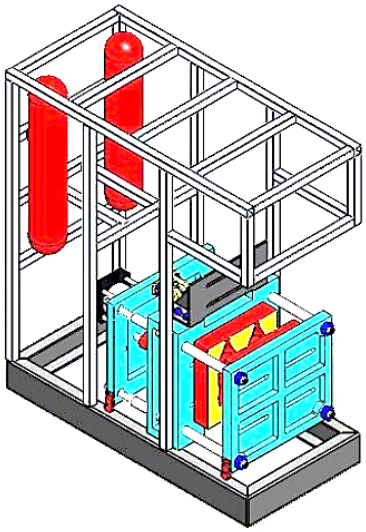

Fig. 2. CAD model of the machine structure

Table 1

PET bottle blowing machine components

1	Frame	7	Front door
2	Side door 1	8	Emergency stop button
3	Side door 2	9	Start switch
4	Side door 3	10	Mold
5	Handle	11	Blower cylinder
6	Roof	12	Manual control area

3. Stress distributions and crack propagation

Many fracture mechanisms remain poorly understood, particularly when it comes to using new materials or innovative processes. The stress distribution near the tip of a crack in a structure is singular: the stress at the crack tip rapidly tends towards infinity. Consequently, unlike cases of holes or cutouts, the stress intensity approach is not applicable for assessing the severity of a cracked structure. In an elastic structure with cracks, the amplitude of the stress at this singularity, also known as the stress intensity factor, is used to evaluate the residual strength of the structure and its ability to resist crack propagation. The theory of linear elastic fracture mechanics (LEFM) is based on the fundamental assumption that the structure remains elastic throughout the fracture process. This approach, based on the stress intensity factor, constitutes a key tool for understanding and modeling the behavior of cracked structures. According to this theory, the following expression governs the stress field near the crack tip [18]:

$$\begin{pmatrix}\sigma_x\\ \sigma_y\\ \sigma_z\end{pmatrix}=\frac{K_I}{\sqrt{2\pi r}}cos\frac{\theta}{2}\begin{pmatrix}1-sin\frac{\theta}{2}sin\frac{3\theta}{2}\\ 1+sin\frac{\theta}{2}sin\frac{3\theta}{2}\\ sin\frac{\theta}{2}sin\frac{3\theta}{2}\end{pmatrix}+\frac{K_{II}}{\sqrt{2\pi r}}cos\frac{\theta}{2}\begin{pmatrix}-sin\frac{\theta}{2}\left(2+cos\frac{\theta}{2}cos\frac{3\theta}{2}\right)\\ sin\frac{\theta}{2}cos\frac{\theta}{2}cos\frac{3\theta}{2}\\ cos\frac{\theta}{2}\left(1-sin\frac{\theta}{2}sin\frac{3\theta}{2}\right)\end{pmatrix} \quad (1)$$

and also:

$$\begin{pmatrix}\tau_{xy}\\ \tau_{yz}\end{pmatrix}=\frac{K_{III}}{\sqrt{2\pi r}}\begin{pmatrix}-sin\frac{\theta}{2}\\ cos\frac{\theta}{2}\end{pmatrix}\ k=1,2,3 \quad (2)$$

Here, r is the distance from the crack tip, and $f_{ij}(\theta)$ is a function describing the angular variation of the stress field. K_I, K_{II}, and K_{III} represent the stress intensity factors for the three modes of opening.

4. Mold closing mechanism

The mold closing mechanism plays a crucial role in the molding process. It allows the mold to be easily installed on the machine, ensuring a smooth opening and closing movement (Fig. 3). The mechanism is designed to provide the high clamping force required for the high-pressure blow molding process. This system ensures that the force is evenly distributed across the mold, guaranteeing optimum blow-molding quality.

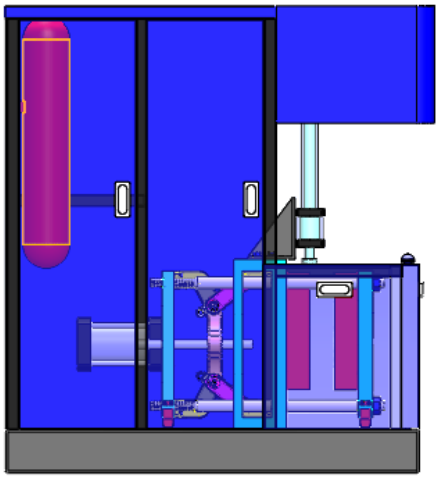

Fig. 3. CAD model of the mold closing mechanism (open mold)

5. Parallel clamping system and the loads acting on the knee bra

The parallel clamping system ensures precise vertical movement of the movable platens and hermetic clamping of the mold (Figure 4).

The locking force is crucial to keep the two halves of the mold hermetically sealed during the preform blow molding process at a pressure of 30 bar.

There are two main forces acting on the clamping mechanism:

Holding force: This force, generated by the pressure of the cylinder piston, keeps the two mold halves firmly clamped.

Blow force: This force, resulting from the process of blowing the preforms, tends to open the mold.

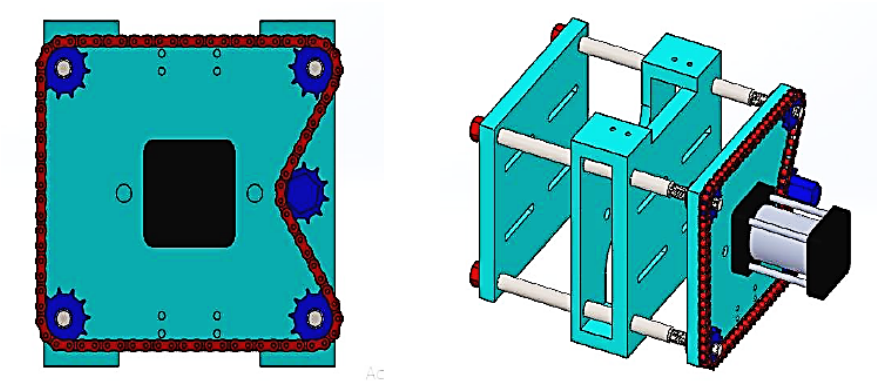

Fig. 4. CAD model of parallel clamping system

5.1 Calculation of cylinder piston force

The piston force (F_1) can be determined from the following formulae using the piston area (A), operating pressure (P) and friction (R) [19].
Piston force (F_1):

$$F_1 = P.A - R$$

$$F_1 = P.\frac{\pi.D^2}{4} - \left(10\%.P.\frac{\pi.D^2}{4}\right) \quad (3)$$

Restoring force (F_2): $F_2 = P.A\left(1 - \frac{d}{D}\right) - R$

$$F_2\left(daN\right) = P.\frac{\pi\left(D-d\right)^2}{4} - R \quad (4)$$

Where:

- D: piston diameter (mm)
- P: operating pressure (bar)
- d: rod diameter (mm)
- R: friction force (≈10%)
- A: piston area (mm^2)
- F_1 and F_2: force on the piston (N)

Our blowing machine uses a double-acting cylinder with a diameter of 80 mm (D=80mm and d=20mm) and an operating pressure of 8 bar.
From these: F_1= 3617.2 N which is the force applied by the cylinder piston on the movable 7 rear platen to close the mold, and F_2= 1413 N that refers to the Mold opening force.

5.2 Calculation of blowing force

The blowing force (F) is a critical parameter in the blow molding process, determined by the following equation:

$$F = P.S \quad (5)$$

In his context, P represents the blowing pressure applied within the mold, while S denotes the half-cavity area of the two cylinders. By multiplying the applied pressure by the cavity area, we can accurately compute the total force exerted on the mold during the preform expansion. This computation is essential for ensuring the mold's ability to withstand internal pressures, thereby preserving the process's efficiency and safety.

To be within the safety zone, we assume a blowing pressure equal to 30 bar (maximum value), and S projected frontal area equal to 0.00255 m² (for a mold of two 2-litre bottles). According to this:

$$F = 30 \times 0.00255 = 7.65 \text{ kN}$$

The force exerted by the compressed air on the mold during blowing is 7.65 kN. To ensure that the mechanism can withstand this force, a static finite element analysis will be carried out. This analysis will determine the stresses, strains and safety coefficient of the system**.**

6. Modeling and simulation procedure

6.1 Knee brace model mesh

All components of the mechanism are fabricated from carbon steel, specifically GS620 cast steel, which possesses minimum yield strength of 620 MPa. The detailed mechanical properties of the material are summarized in Table 2.

Table 2

Properties of mechanism elements

Property	**Value**	**Unit**
Young's modulus	210	GPa
Poisson's Ratio	0.28	S.U.
Shear Modulus	79	GPa
Density	7700	Kg/m^3
Tensile Strength	723.82	MPa
Yield Strength	620.42	MPa
Coefficient of Thermal Expansion	$1.3e^{-005}$	/k
Thermal Conductivity	50	W/(m.k)

Meshing is carried out automatically in the ANSYS software, which includes an integrated automatic mesh (Fig. 5). Using the options available, we freely applied choices to the segments and surfaces with a refinement of 1 mm to the contact zone, and the result is:

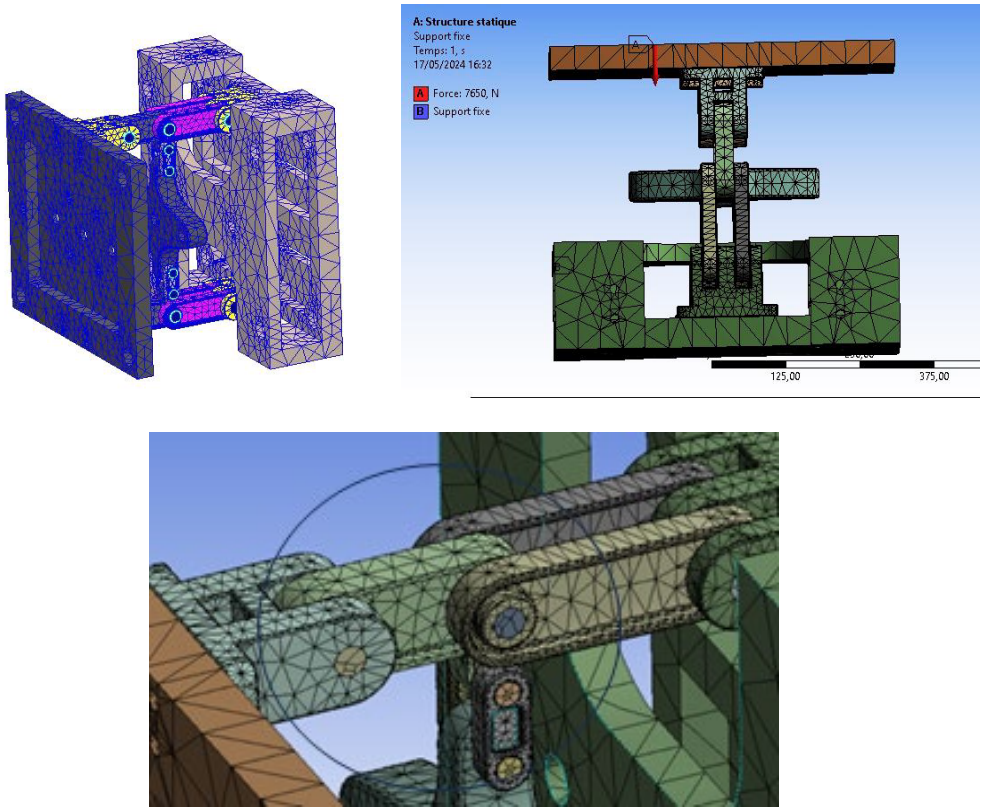

Fig. 5. Meshing of the Mold Closing Mechanism

6.2 Boundary conditions

Fig. 6 illustrates the boundary conditions applied to the geometric model:
A fixed support is applied to the base platform, preventing any displacement or rotation.
A force of 7650 N is exerted on the mobile rear plate, distributed symmetrically with F/4 applied at each corner as shown.
The central driving force F_1 is also applied along the axis of the mechanism
These boundary conditions are intended to replicate the actual mechanical loading scenario and constraints during operation.

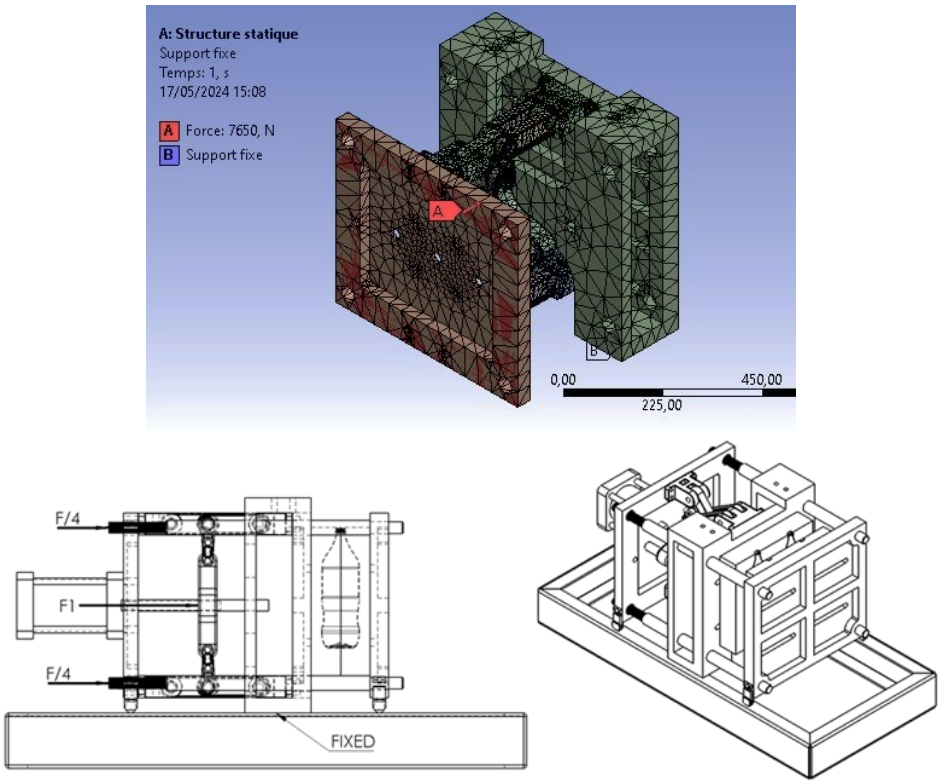

Fig. 6. Boundary conditions

7. Results and discussions

7.1 Constraints (von Mises)

Assuming an isotropic material, this stress is invariant to changes in reference frame, which means that it must be expressed in terms of the invariants of the 'stress tensor' [20].

$$\sigma = \begin{pmatrix} \sigma_x & \tau_{xy} & \tau_{xz} \\ \tau_{yx} & \sigma_y & \tau_{yz} \\ \tau_{zx} & \tau_{zy} & \sigma_z \end{pmatrix} \tag{6}$$

The invariants of the stress tensor are given by:

$$I_1 = Tr(\sigma) = \sigma_x + \sigma_y + \sigma_z \tag{7}$$

$$I_2 = \sigma_x\sigma_y + \sigma_y\sigma_z + \sigma_z\sigma_x - \tau_{xy}^2 - \tau_{yz}^2 - \tau_{zx}^2 \tag{8}$$

$$I_3 = \sigma_x\sigma_y\sigma_z + 2\tau_{xy}\tau_{yz}\tau_{xz} - \sigma_x\tau_{yz}^2 - \sigma_y\tau_{zx}^2 - \sigma_z\tau_{xy}^2 \tag{9}$$

The equivalent von Mises stress is obtained from the second invariant of the deviatoric stress tensor. The invariant I_2 given by equation (8) is a general expression based on the components of the stress tensor.

However, in the case of the von Mises criterion, we must use the second invariant of the deviatoric stress tensor, which is given by:

$$J_2 = \frac{1}{6}\left[\left(\sigma_x - \sigma_y\right)^2 + \left(\sigma_y - \sigma_z\right)^2 + \left(\sigma_z - \sigma_x\right)^2\right] + \left[\tau_{xy}^2 + \tau_{yz}^2 + \tau_{zx}^2\right] \tag{10}$$

Since the von Mises stress is derived from the deviatoric stress tensor, it is directly related to J_2:

$$\sigma_{eq} = \sqrt{3J_2} \tag{11}$$

Replacing J_2 in the expression for the equivalent stress, we obtain:

$$\sigma_{eq} = \sqrt{0.5\left[\left(\sigma_x - \sigma_y\right)^2 + \left(\sigma_y - \sigma_z\right)^2 + \left(\sigma_z - \sigma_x\right)^2\right] + 3\left[\tau_{xy}^2 + \tau_{yz}^2 + \tau_{zx}^2\right]} \tag{12}$$

This expression is used in the analysis of ductile isotropic materials to determine whether a material reaches its plastic state under a given stress state.

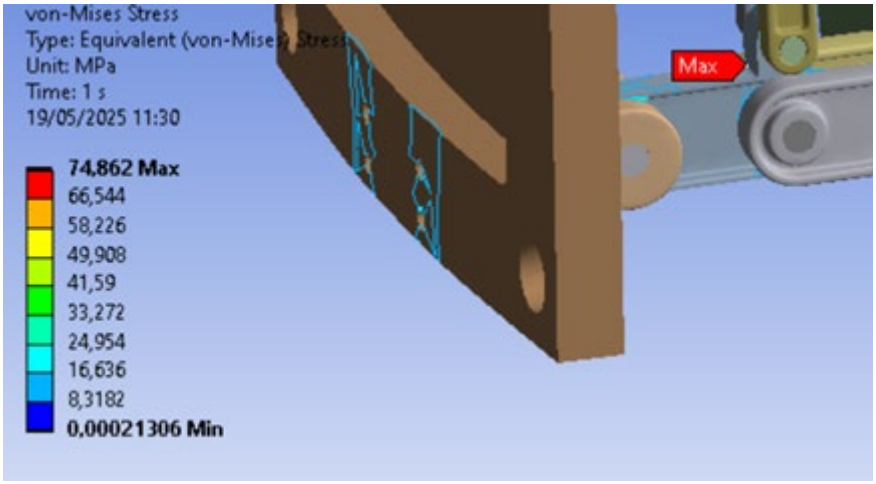

Fig. 7. Von Mises constraint

The advantage of the von Mises criterion is that it simplifies the analysis of the results: instead of concentrating on the stress and shear forces in all directions. Fig. 7 shows the stress distribution when we apply a force of 7650 N. The mechanism is primarily subjected to compressive loading. The highest concentration of stress occurs in the middle component, which serves as the interface between the fixed and mobile plates. As shown in the figure, the maximum equivalent von Mises stress reaches 74.862 MPa, located at the connection zone between this central part and the adjacent components. In

contrast, the rest of the structure experiences significantly lower stress levels, indicating that the load is not evenly distributed throughout the mechanism. This localized stress must be carefully considered in the design to avoid potential failure or fatigue over time.

7.2 Deformation

Applying a force of 7650 N to the mechanism generates the deformations shown in Figure 8. The strain scale shows negative values, indicating compressive loading. The minimum strain recorded is -3.28×10^{-6} and the maximum value is 185×10^{-6}.

Analysis of the deformations shows that all the parts of the mechanism were able to withstand the stresses applied. The deformation values observed remains within acceptable limits, confirming the judicious choice of material for the manufacture of the knee brace.

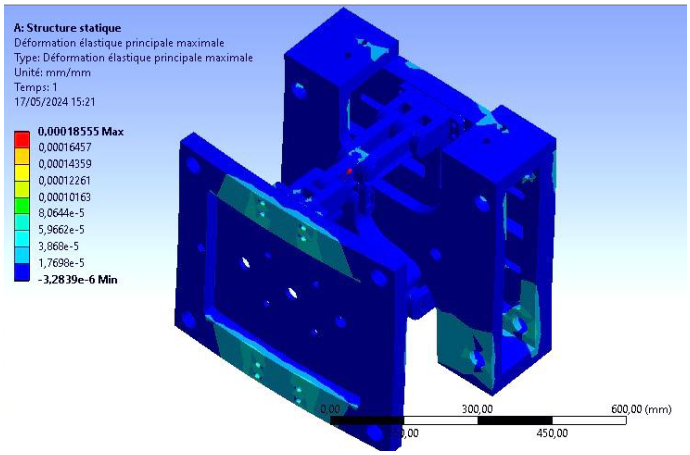

Fig. 8. Principal Deformation Analysis

7.3 Displacement

Fig. 9 shows the displacement of the various parts of the locking mechanism following the application of the locking force. It can be seen that the maximum displacement is 0.208 mm and the minimum displacement is 0 mm.

The maximum displacement occurs at the plate carrying the cylinders, on the sides of the two guiding columns. However, this displacement remains minimal and has no impact on the proper functioning of the machine.

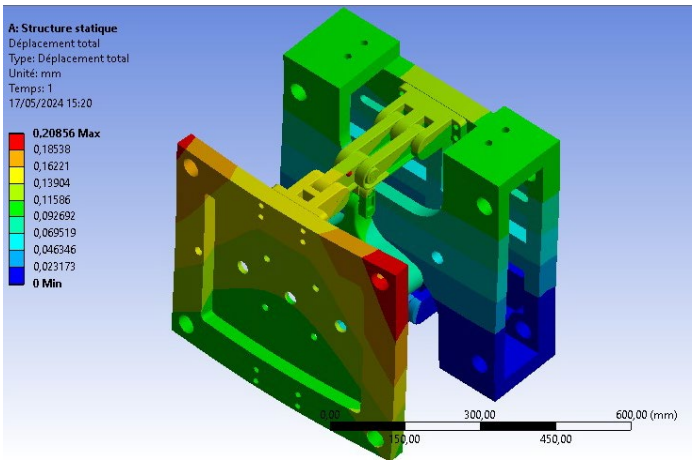

Fig. 9. Displacement Analysis

7.4 Safety Factor

The purpose of the safety factor is to provide a margin of safety between theoretical calculation and practical application. In theory, to give the material certain strength, it should withstand stresses that do not exceed the yield strength (to avoid permanent plastic deformation). However, in practice, the yield strength may not be completely theoretically considered, meaning there are defects in the material that can cause additional stress [20]. In static loading conditions, the factor of safety (S) helps ensure that the structure or component can support the applied loads without failure. It's a measure of how much stronger the system is compared to the expected maximum load or stress.

The safety factor S is calculated as:

$$S = \frac{\sigma_{\text{lim}}}{\sigma_{\text{max}}} \tag{13}$$

According to Figure 10, the safety factor of the most stressed parts, as illustrated in the figure, ranges between 15 and 3.339. This indicates that the design is robust and the chosen material is adequate.

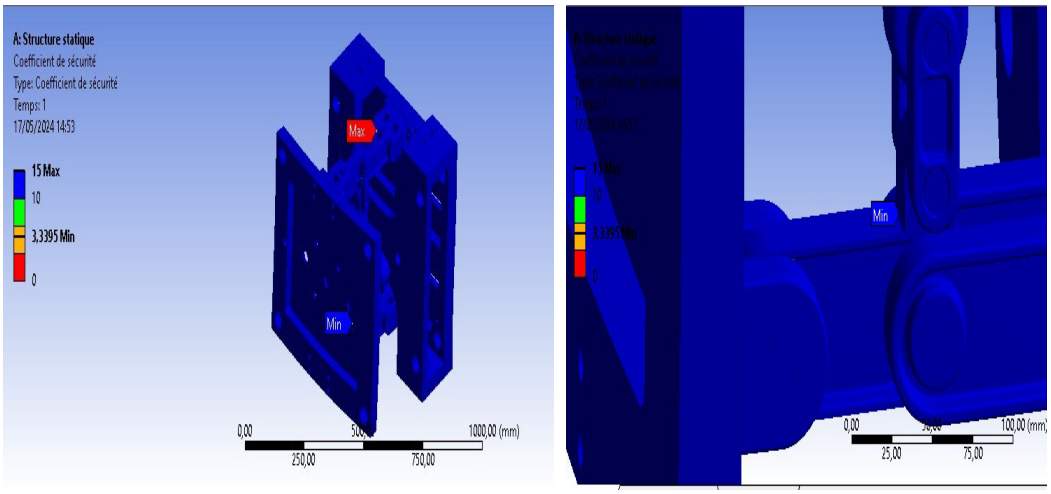

Fig. 10. Analysis of the safety factor

The central piece undergoes significant compressive force, resulting in a safety factor of 3.339. Since this piece is subjected to cyclic loads, it is crucial to assess its fatigue strength as well as the stress intensity factor generated by an elliptical crack present on its surface.

7.5 Crack sizing

The locking mechanisms of PET bottle blow molding machines are frequently prone to cracks, which can seriously disrupt production.

Potential causes of elliptical Cracks:

• Repeated cyclic stresses, inherent in the operation of PET blow molding machines, cause material fatigue, leading to the formation of elliptical cracks.

• Significant vibrations generated by these machines can also induce cracks, particularly at fastening points and in stress concentration areas.

• Material defects or machining errors can create weak points conducive to crack formation.

Characteristics of elliptical Cracks:

• Elliptical cracks are often indicative of cyclic stresses or manufacturing defects.

• Their shape reveals the direction of stresses and crack propagation.

• Their size varies, ranging from microcracks undetectable to the naked eye to cracks exceeding 5 mm.

This study aims to examine the behaviour of an elliptical crack in a locking mechanism part subjected to maximum stress during the blowing operation (Figure 11). This geometry is commonly used in fracture mechanics, as illustrated in references [20, 21].

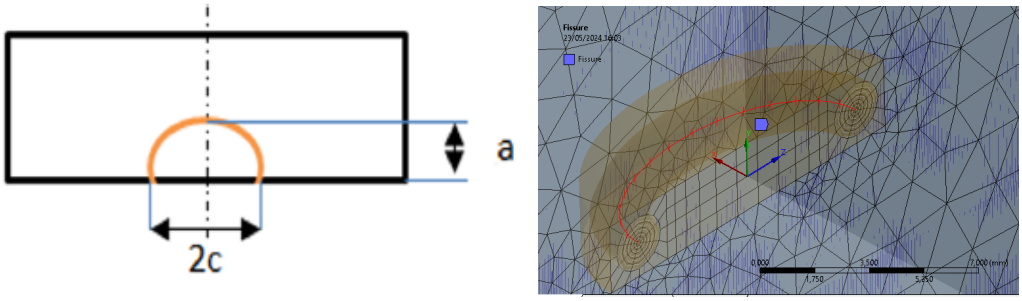

Fig. 11. Shape and Dimension of the Crack

The software allows defining the parameters of this crack by entering the length of the semi-major axis (c) and the semi-minor axis (a). For this study, we have chosen c = 5 mm and a = 3 mm.

The meshing process was automated using the built-in meshing system of the ANSYS software. By exploiting the available options, we were able to refine and precisely select the segments and surfaces, paying particular attention to the contact area where a fine mesh of 1 mm was applied with 262509 nodes and 170731 elements (Figure 12).

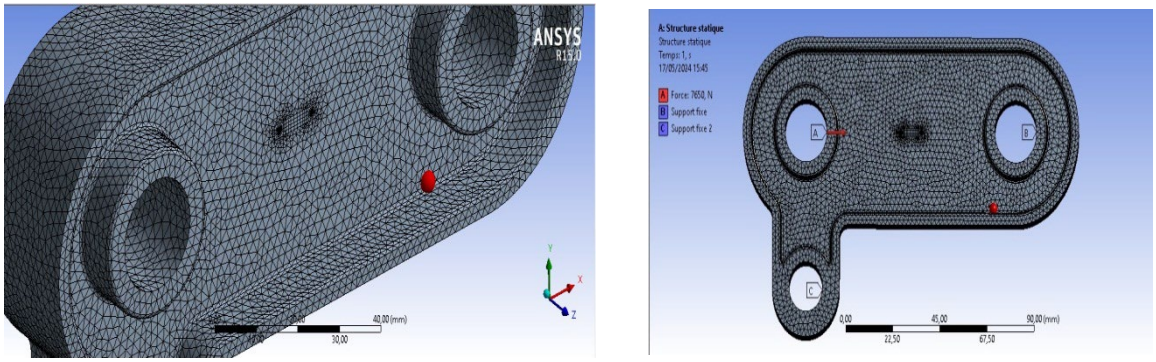

Fig. 12. Position of crack on workpiece

7.6 Stress Intensity Factor

The stress intensity factor (K_I) is a crucial parameter for evaluating the fracture resistance of structural components. In the case of an elliptical crack in a piece of carbon steel (GS620) subjected to compressive force, finite element analysis (FEA) in ANSYS allows for precise determination of (K_I).

The geometry of the piece and the elliptical crack was modeled using ANSYS software. The dimensions of the piece, the length (a), and the depth (c) of the crack, as well as the orientation of the crack, must be accurately defined.

An appropriate mesh is generated using tetrahedral elements, depending on the complexity of the geometry. Mesh refinement is applied in the crack zone to capture significant stress gradients.

The compressive force applied to the piece is defined as a boundary condition. Restraint or symmetry conditions can be applied to other surfaces of the piece.

Finite element analysis is performed using an appropriate solver in ANSYS. The solution provides stress and strain fields in the piece as well as the stress intensity field at the crack, in our case, the maximum value is found at the centre of the crack as shown in figure 13, which is due to compression.

Based on Figure 13, which illustrates the variation of the stress intensity factor K_I, the maximum value is observed at the center of the crack and is equal to 3.7553 MPa.mm$^{-0.5}$. This result provides a clear indication of the stress concentration near the crack's midpoint, as further supported by the data presented in Figs. 13 and 14. A high value of K_I reflects a significant stress concentration zone, which considerably increases the risk of crack propagation and potential structural failure of the component.

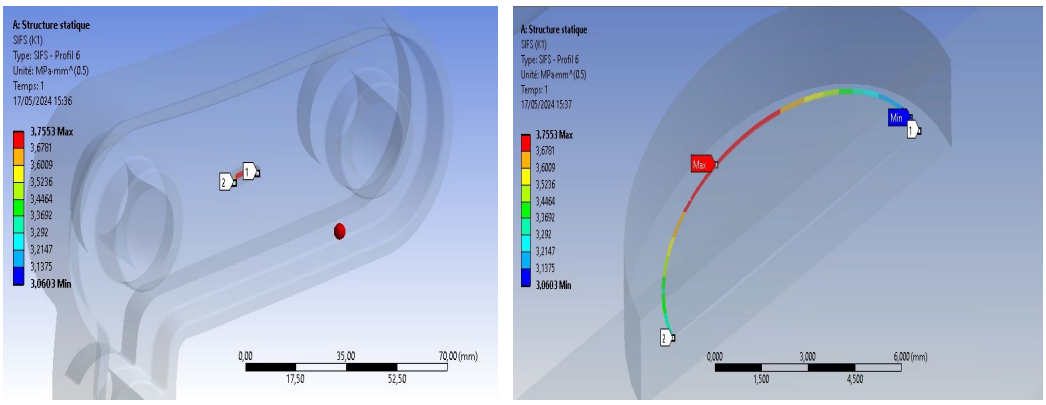

Fig. 13. Stress intensity factor K_I

Fig. 14 illustrates the variation of the stress intensity factor (SIF) as a function of the crack width (2c). It is observed that the SIF increases progressively with the enlargement of the crack, indicating a higher stress concentration at larger crack sizes. The maximum value of the SIF is located at the center of the crack, which can be attributed to the applied compressive loading.

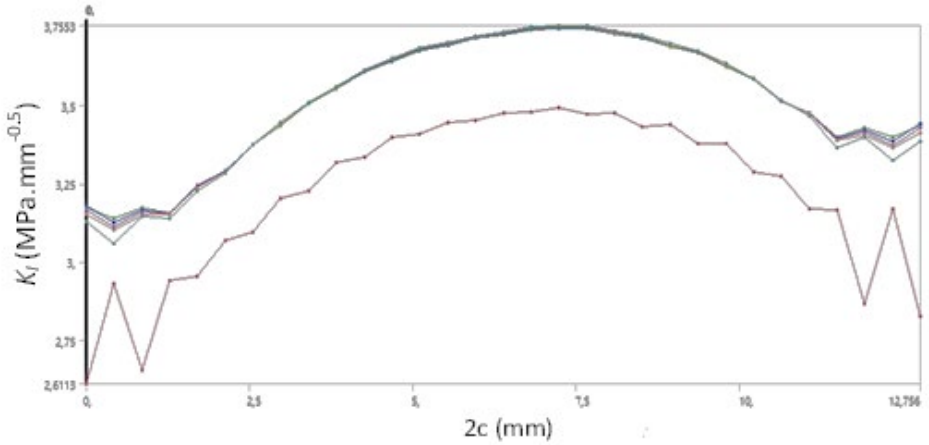

Fig. 14. Variation of the stress intensity factor K_I as a function of the crack width $2c$

7.7 Fatigue Influence

The evaluation of the fatigue of the junction part which is mainly subjected to a compressive load which is worth 76500 N which represents the locking force of the mechanism of the blowing machine to guarantee its durability and safety during operation. Using ANSYS finite element (FE) simulation tools, it is possible to analyze the behavior of the part under cyclic loading and predict its service life and percentage of damage.

Fig. 15 illustrates the impact of mean stress on fatigue life using different correction models, including Goodman, Soderberg, and Gerber criteria. The upper plot shows a typical cyclic load of constant amplitude with alternating stress values, simulating the operational loading conditions experienced by the part.

The lower diagram presents the mean stress correction theory, which is crucial in fatigue analysis. Among the models shown:

The Goodman line (linear), represented in green, provides a conservative estimate for ductile materials, correlating the alternating stress with the mean stress and the material's ultimate strength.

The Soderberg criterion is more conservative and uses the yield strength as a limit.

The Gerber curve is a parabolic approximation that is less conservative than Goodman and more accurate for certain ductile materials.

These criteria are used to evaluate whether the combination of mean and alternating stresses falls within the safe fatigue zone. If a point lies under the chosen curve, the material is considered safe against fatigue failure for the given stress cycle.

Post-processing results from the fatigue analysis, when interpreted using these correction models, allow engineers to estimate residual life, assess damage

accumulation, and implement design improvements to extend the service life and reliability of the component.

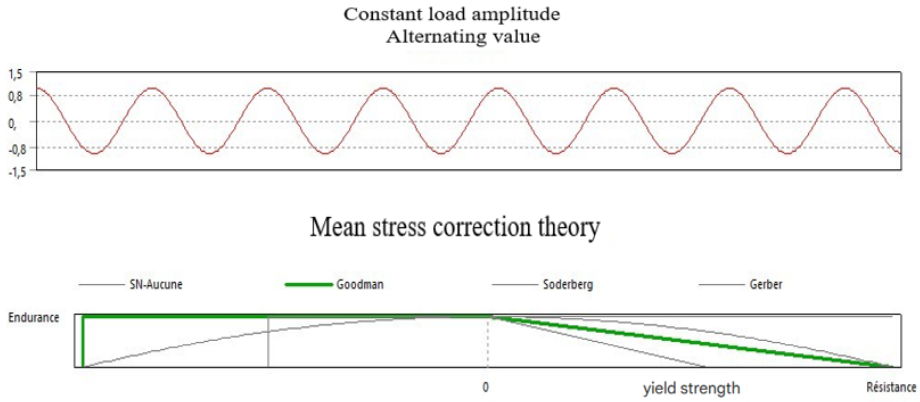

Fig. 15. Correction of average stress Goodman's law

7.8 Life span

The lifespan of a component refers to the maximum number of load cycles it can endure before failing due to fatigue. It is usually expressed in terms of cycles or operating hours, depending on the context. As illustrated in figure 16, the maximum lifespan of the component in question is 10^6 cycles.

Figures 17 and 18 collectively provide insight into the fatigue performance and safety of the mechanism. Figure 17 highlights the critical area where damage accumulation is most pronounced, specifically at the junction part under study, which is subjected to repeated stress cycles. The rest of the mechanism exhibits negligible damage, indicating that it remains structurally sound under operational conditions.

The calculation of the safety factor (S) in fatigue is crucial to ensure the durability of structures subjected to cyclic loads. Several criteria are used to combine the effects of alternating stress (σ_a) and mean stress (σ_m) in fatigue analysis. The most commonly applied failure criteria include:

- ***Goodman Criterion*:**

This is a linear relationship that assumes the endurance limit decreases linearly with increasing mean stress. The safety factor S is calculated as:

$$S = \frac{S_e}{\sigma_a + \frac{\sigma_m S_e}{\sigma_u}} \tag{14}$$

where:

σ_a : alternating stress

σ_m : mean stress

S_e : endurance limit
σ_u : ultimate tensile strength

- ***Soderberg Criterion:***

A conservative approach that uses the yield strength instead of the ultimate strength:

$$S = \frac{S_e}{\sigma_a + \frac{\sigma_m S_e}{\sigma_y}} \tag{15}$$

where σ_y is the yield strength.

Fig. 18 presents the distribution of the safety factor under fatigue loading. The minimum value recorded is 2.07, which, although reduced due to fatigue effects, still represents an acceptable level of safety. This reduction reflects the material's diminished resistance caused by microstructural degradation over time, yet it remains within acceptable design limits to prevent failure.

In summary, while localized fatigue damage is present, particularly in the junction area, the overall structural integrity is preserved, and the safety factor remains within an acceptable range, ensuring reliable performance throughout the mechanism's service life.

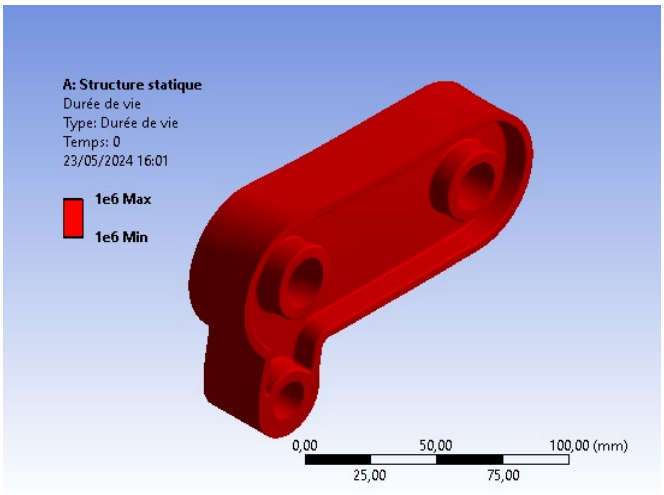

Fig. 16. Component Life Span 10^6 max Cycles

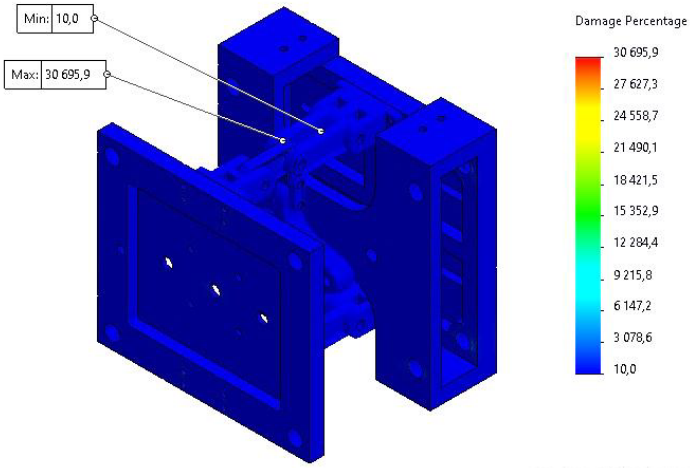

Fig. 17. Percentage of Damage in the Mechanism

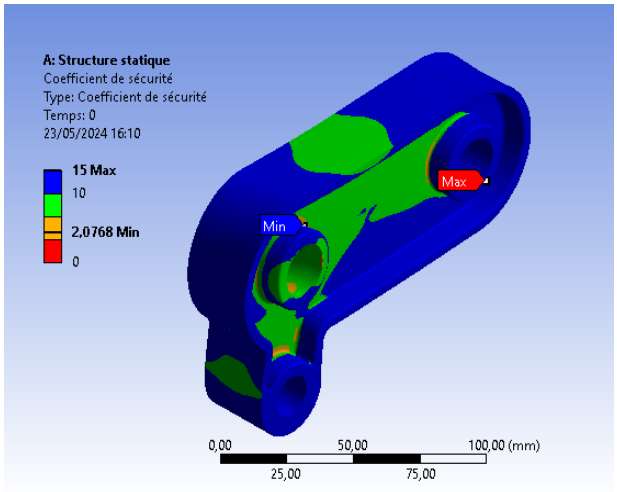

Fig. 18. Safety Factor under Fatigue

8. Conclusion

This project involves a study of the strength of the locking mechanism of a PET bottle mold on a semi-automatic blow-molding machine. The mold has two cavities, each with a capacity of 2 litters. The study focused on the ability of the mechanism's components to withstand a static load of 7650 N generated by the mold locking forces. Firstly, we found that the mechanism's minimum safety coefficient is 3.339. This coefficient is the lowest located in the junction piece between the plate and the side elements of the mechanism. This result indicates that the part is the most stressed and that it is important to check its fatigue strength. As the part is subjected to cyclic loading, we decided to carry out a

fatigue study to assess its resistance to this phenomenon. Finite element simulation is used to identify the areas of the part that are subject to the greatest stress and most likely to undergo fatigue failure. This makes it possible to target design and inspection efforts on these critical areas. We carried out a study on an elliptical crack of dimensions 5 mm x 3 mm, located at the center of the surface of the part.

We found a stress intensity factor K of 3.7553 $MPa.mm^{-0.5}$ at the center of the crack, due to compressive stresses.

The Fatigue Tool module in ANSYS Workbench is used to evaluate the fatigue behavior of components subjected to cyclic loading. It calculates both the fatigue life (i.e., the number of cycles to failure) and the safety factor (*S*) based on user-defined loading conditions and material properties.

In this analysis, the Goodman criterion is employed to account for the combined effects of alternating and mean stresses. This criterion provides a conservative estimation of fatigue failure, especially useful for ductile materials. In the present context, a fatigue life of one million cycles (10^6) is considered the acceptable threshold for safe operation.

The safety factor in fatigue is the ratio between the material's fatigue strength and the applied stress levels. For instance, a computed safety factor of 2.0768 indicates that the component can theoretically endure stress levels 2.0768 times higher than those currently applied before experiencing fatigue failure. A higher safety factor typically implies better resistance to fatigue damage and a more reliable design.

Ansys Workbench allows visualization of critical areas of the part, where the fatigue life is minimal and the risk of failure is maximal.

In this study, the analysis focused on a single crack size and location. Further research with varying crack dimensions and positions could provide a more comprehensive understanding of fatigue behavior. While material properties were considered, incorporating environmental factors (e.g., temperature fluctuations) could refine the fatigue assessment. For future work, we recommend: Conducting fatigue tests on physical samples to compare and validate finite element simulation results. Investigating design modifications (e.g., material selection, geometry adjustments) to improve the fatigue resistance of the locking mechanism.

REFERENCES

[1]. *M. Bordival*, "Modelisation et optimisation numerique de l'etape de chauffage infrarouge pour la fabrication de bouteilles en PET par injection-soufflage", Ph.D. thesis, Ecole Nationale Superieure des Mines de Paris, 2009.

[2]. *S. Patterson, Y. C. Ho, W. C. Wang*, "The effect of cyclic loading on the mechanical performance of surgical mesh", in: EPJ Web of Conferences, **vol. 6**, EDP Sciences, 2010, pp. 21007.
[3]. *P. O. Judt, A. Ricoeur,* "Crack growth simulation of multiple cracks systems applying remote contour interaction integrals", Theoretical and Applied Fracture Mechanics, **vol. 75**, 2015, pp. 78–88.
[4]. *P. H. O'Hara, J. Hollkamp, C. A. Duarte, T. Eason*, "A two-scale generalized finite element method for fatigue crack propagation simulations utilizing a fixed, coarse hexahedral mesh", Computational Mechanics, **vol. 57**, 2015, pp. 55–74.
[5]. *R. G. Forman, V. Shivakumar, J.W. Cardinal, L.C. Williams, P.C. McKeighan*, "Fatigue Crack Growth Database for Damage Tolerance Analysis", Final report, Springfield, Virginia, 2005.
[6]. *J.J. Marigo*, "Modelling of brittle and fatigue damage for elastic material by growth of microvoids", Engineering Fracture Mechanics, **vol. 21**, no. 4, 1985, pp. 861-874.
[7]. *C. Chow, Y. Wei*, "A model of continuum damage mechanics for fatigue failure", International Journal of Fracture, **vol. 50**, 1991, pp. 301–316.
[8]. *J. Lemaitre*, "A Course on Damage Mechanics", Springer, Berlin,1992.
[9]. *J. Fish; C. Oskay*, "A Nonlocal Multiscale Fatigue Model", Mechanics of Advanced Materials and Structures, **vol. 12**, no. 6, 2005, pp. 485–500.
[10]. *J. Schijve*, "Fatigue of Structures and Materials", 2nd Edition, Springer, 2009.
[11]. *M.J. Borden, T.J.R. Hugher, C.M. Landis, C.V. Verhoosel*, "A higher-order phase-field model for brittle fracture: Formulation and analysis within the isogeometric analysis framework", Computer Methods in Applied Mechanics and Engineering, **vol. 273**, 2014, pp. 100–118.
[12]. *C. Miehe, F. Welschinger, M. Hofacker*, "Thermodynamically consistent phase-field models of fracture: Variational principles and multi-field FE implementations", International Journal for Numerical Methods in Engineering, **vol. 83**, no. 10, 2010, pp. 1273–1311.
[13]. *M.J. Borden, T.J.R. Hugher, C.M. Landis, A. Anvari, I.J. Lee*, "A phase-field formulation for fracture in ductile materials: Finite deformation balance law derivation, plastic degradation, and stress triaxiality effects", Computer Methods in Applied Mechanics and Engineering, **vol. 312**, 2016, pp. 130–166.
[14]. *C. Kuhn, T. Noll, R. Müller*, "On phase field modeling of ductile fracture", GAMM-Mitteilungen, **vol. 39**, 2016, pp. 35–54.
[15]. *F. Aldakheel, P. Wriggers, C. Miehe*, "A modified Gurson-type plasticity model at finite strains: formu lation, numerical analysis and phase-field coupling", Computational Mechanics, **vol. 62**, 2017, pp. 815–833.
[16]. *S. Teichtmeister, D. Kienle, F. Aldakheel, M.A. K*eip, "Phase field modeling of fracture in anisotropic brittle solids, International Journal of Non-Linear Mechanics, **vol. 97**, 2017, pp. 1–21.
[17]. *C. Schreiber, C. Kuhn, R. Mülle, T.i Zohd*, "A phase field modeling approach of cyclic fatigue crack growth", International Journal of Fracture, **vol. 225**, 2020, pp. 89–100.
[18]. *H.A. Richard; M. Fulland; M. Sander*, "Theoretical crack path prediction", Fatigue Fracture of Engineering Materials and Structures, **vol. 28**, no.1-2, 2005, pp. 3–12.
[19]. *C. Michaud*, "Vérins pneumatiques: pression-effort", Edition 1.1, Unknown Publisher, 2009, p. 71.
[20]. *R. C. Shah, A. S. Kobayashi*, "Stress intensity factor for an elliptical crack under arbitrary normal loading", Engineering Fracture Mechanics, **vol. 3**, 1971, pp. 71–96.
[21]. *J. C. Newman; I. S. Raju*, "An empirical stress-intensity factor equation for the surface crack", Engineering fracture mechanics, **vol. 15**, no. 1-2, 1981, pp. 185–192.